ARTICLE NO. 78-956R

Design and Experimental Studies of a Type A V/STOL Inlet

H. C. Potonides, * R.A. Cea† and T. F. Nelson‡
Grumman Aerospace Corporation, Bethpage, N. Y.

Design and experimental studies have been conducted to evolve a high performance, high incidence capability inlet for subsonic V/STOL applications. Design criteria, including effects of the flight control system on the inlet requirements, were selected to satisfy both low and high speeds. Based on these studies, several inlets were designed, fabricated and tested in the Grumman Low Speed Tunnel. Inlet performance and separation bounds were determined. The baseline inlets with a long centerbody met their respective design goals, and exceeded the performance and incidence capability of inlets of equal area contraction ratio. At the design power/nacelle tilt requirements, matched pressure recovery is better than 0.995 with less than 4% distortion.

Nomenclature

A = area
a/g = acceleration ratio
CR = contraction ratio, $(D_H/D_T)^2$
D = diameter
L = length
L_R = lip thickness ratio, $X_T Y'_T/R_T^2$
M = Mach number
p = static pressure
P_T = total pressure
q = dynamic pressure
R = radius
R_N = Reynolds number
T_C = total thrust coefficient, (thrust at α = 0 deg)/qA_2
TR = fraction of gross thrust
V = velocity
W_C = airflow at diffuser exit corrected to standard conditions
X = longitudinal dimension from inlet leading edge
Y = vertical dimension from highlight radius to cowl wall
α = angle of attack, deg
δ_j = nacelle deflection, deg
ψ = yaw angle, deg

Subscripts

DD = drag divergence
DES = design
F = fan
H = highlight
INL = inlet
max = maximum
min = minimum
NAC = nacelle
O, OO = freestream
OP = operating
S = surface
SEP = separation
T = throat
X = at station
1, 2 = inlet designation
2 = fan face or diffuser exit
′ = used with Y_T to denote total lip thickness at the throat station

Received July 10, 1978; presented as Paper 78-956 at the AIAA/SAE 14th Joint Propulsion Conference, Las Vegas, Nev., July 25-27, 1978; revision received Sept. 16, 1978.

Index categories: Subsystem Design; Nonsteady Aerodynamics; Airbreathing Propulsion.

*Propulsion Group Specialist, Fluid Mechanics. Associate Fellow AIAA.
†Project Engineer, V/STOL Propulsion.
‡Senior Engineer, Fluid Mechanics.

Introduction

The flow environment at the inlet of a V/STOL aircraft can be very severe due to heavy crosswind at very low forward speeds, large upwash from the forebody/wing flowfield during aircraft high-lift operation and, for some aircraft configurations, tilting the engine nacelles for lift-assist during takeoff and landing. These flow conditions, and the inlet elements affected, are depicted in Fig. 1.

To provide efficient, steady airflow to the engine during these conditions, the inlet and its components must be tailored to avoid flow separation, which, in addition to performance losses, may cause fan and compressor stall, increased blade stresses and increased noise levels. The various kinds of internal separation that may develop are shown in Fig. 2. Similarly, flow separation can occur externally with attendant drag losses in cruise. Therefore, understanding the mechanisms producing flow separation, and knowledge of the effects that various geometric/operational parameters of an inlet system have on flow separation, both internally and externally, are key elements to a successful inlet design which will meet both low and high speed requirements. Consequently, the inlet design cycle begins with a parametric evaluation of the geometric and operational factors vis-a-vis the design requirements. In the specific case of tilt nacelle configurations, the emphasis is aimed at the selection of design factors resulting in separation-free operation at the most critical flight condition, namely transition landing. These selected factors, together with parameters significant to external flow are cross-evaluated to assess impact on cruise, loiter and engine-out climb drag.

This paper presents Grumman's application of this design philosophy in selecting, testing and properly blending experimentally proven inlet parameters and features to evolve a separation-free, high angle-of-attack capability inlet system for Design 698 V/STOL aircraft.

Inlet Design Requirements

Grumman's conceptual approach to the U. S. Navy Type A V/STOL aircraft, shown in Fig. 3, has twin tilting nacelles,

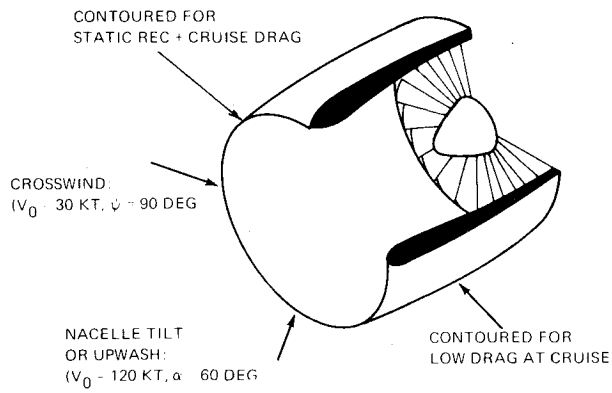

Fig. 1 Inlet design and control.

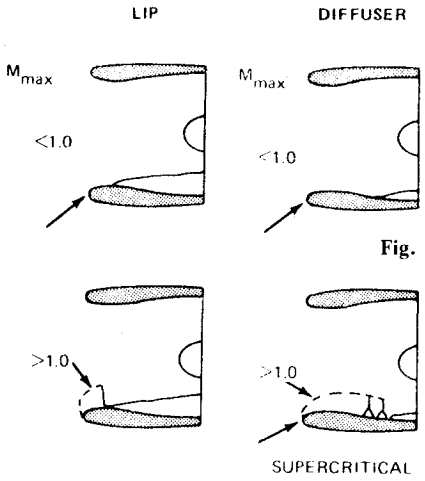

Fig. 2 Kinds of separation.

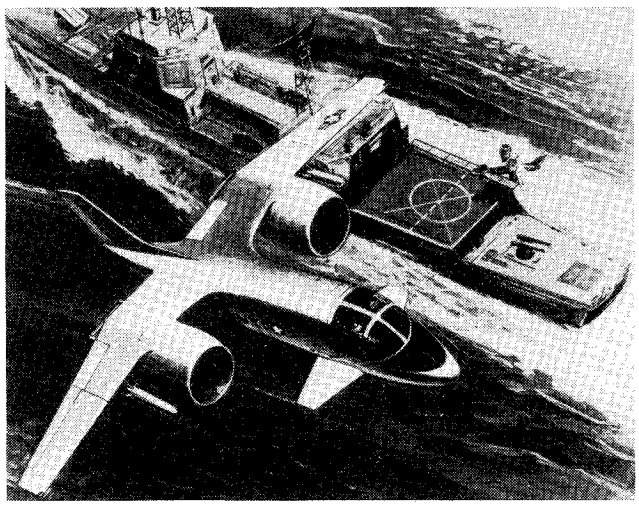

Fig. 3 Conceptual subsonic V/STOL.

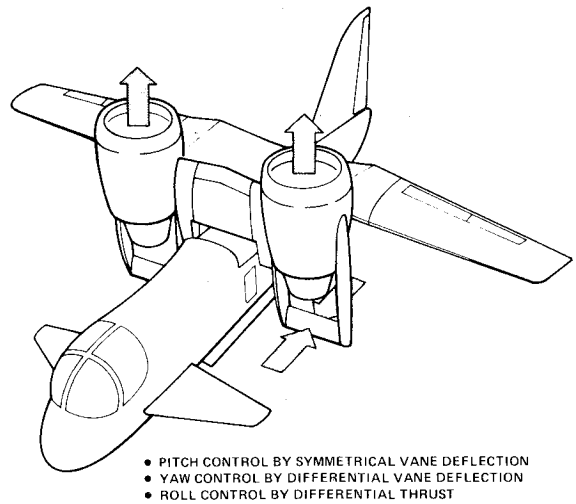

Fig. 4 Vertical flight control.

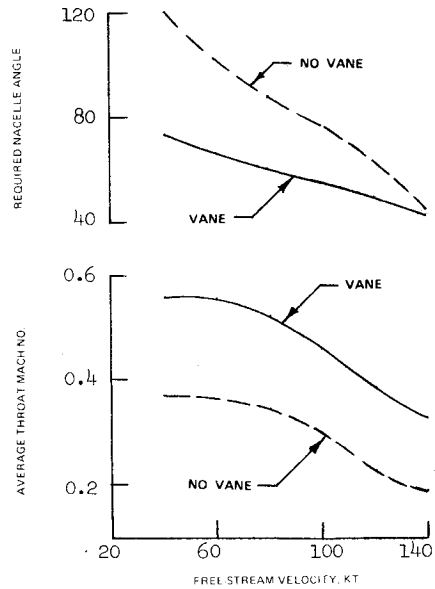

Fig. 5 Effect of control system on inlet requirements.

which incorporate the powerplant and control vanes in the fan stream to provide all VTOL functions—propulsive thrust, thrust modulation and control about all three axes, (schematically shown in Fig. 4). As a result, the inlet flow environment is quite severe during take-off and landing transition. Yet the inlet must provide stable and efficient flow to the engine.

The severity of the flow environment is strongly influenced by the aircraft configuration and its selected control system. The issue of tilt nacelles versus vectored nozzle configurations with their peculiar problem areas, and how these could affect the inlet flow conditions, is adequately debated in the V/STOL literature. What is known, however, is that angle-of-attack capability requirements for twin tilting nacelles with vane control, as incorporated in Grumman's Design 698 A V/STOL aircraft, are substantially lower than the requirements for tilting nacelles without vane control as shown in Fig. 5. Consequently, our inlet problem, though by no means small, is amenable to reasonable design solution.

The specified Design 698 inlet requirements are in summary:

1) High speed—the inlet shall have low drag at cruise Mach of 0.75. This implies a drag divergence Mach number, $M_{DD} \geq 0.75$.

2) Low speed—the inlet shall operate separation-free, with high total pressure recovery and low distortion at the most critical landing transition of the aircraft.

From the inlet design standpoint, the critical operation condition, at any given speed, would be minimum thrust requirement at maximum nacelle deflection. As indicated, in Fig. 6, by the landing transition characteristics of an aircraft not employing flaps, this critical operating requirement occurs in a glide with a negative flight path acceleration. It must be emphasized that the severity of this critical landing transition is not only influenced by the selected control system,

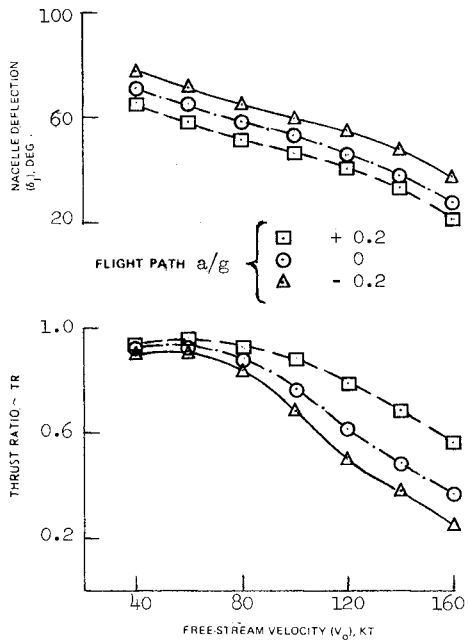

Fig. 6 Landing transitions.

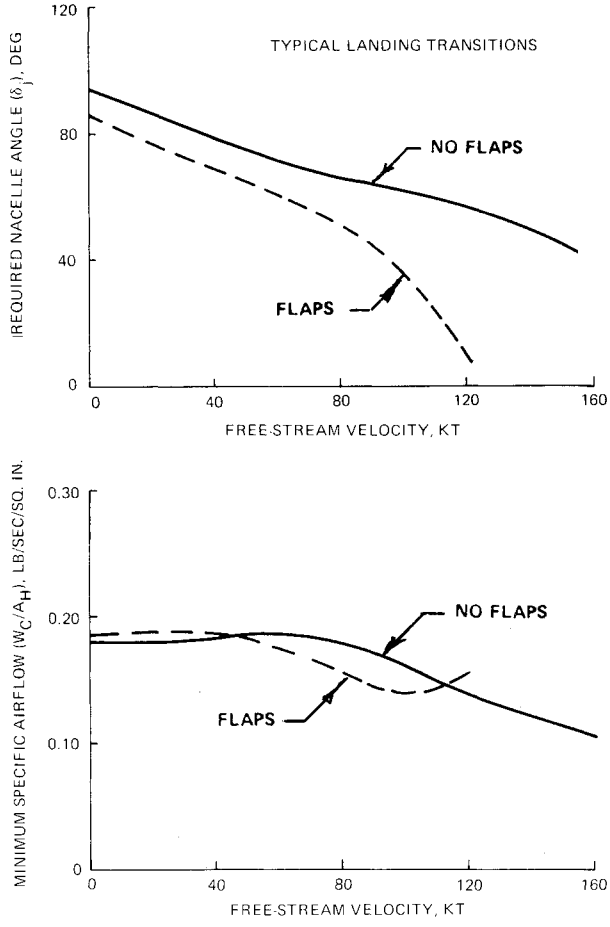

Fig. 7 Inlet low-speed design requirements.

shown earlier in Fig. 5, but also by the aircraft flight configuration, as shown by the comparison, on Fig. 7, between an aircraft landing with and without the use of flaps.

Inlet Design Parameter Selection

Grumman has correlated pertinent NASA and industry data showing the interrelationships of the various geometric

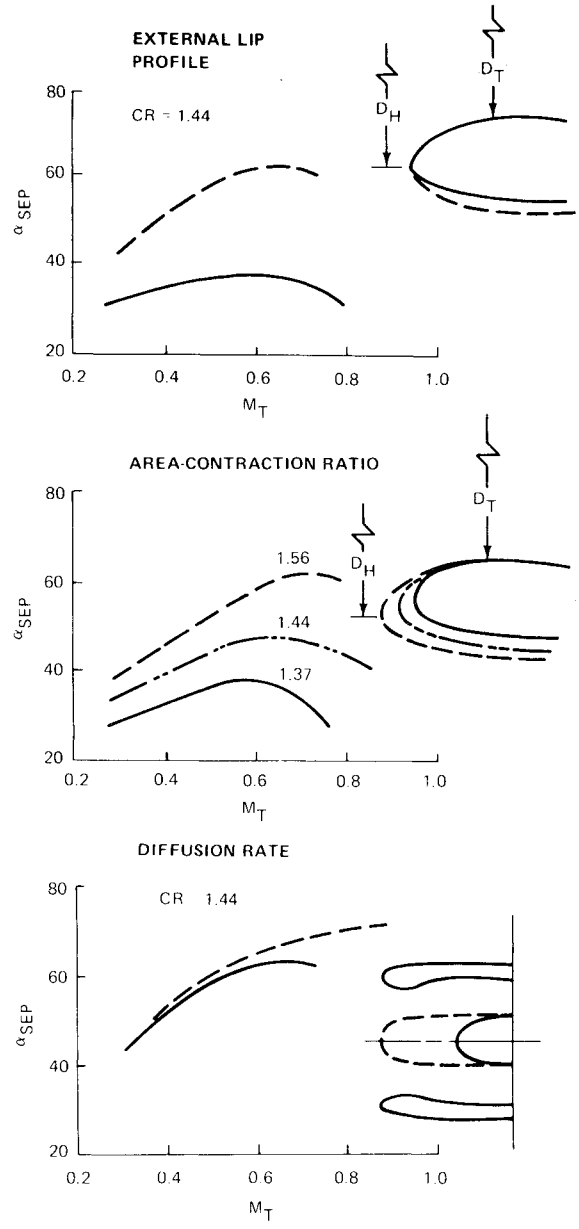

Fig. 8 Selection of low-speed parameters.

and flow parameters as they affect angle-of-attack capability at low speed and drag at cruise. Typical summaries of these correlations are presented below, to highlight some observations and to indicate the compromises the inlet designer must make to satisfy both low and high speed requirements.

Low Speed

Figure 8 indicates that the angle-of-attack capability of an inlet system improves with

1) An increase in the area contraction ratio, A_H/A_T. Large local wall diffusion angles can, however, limit this trend, as indicated by the data of Ref. 1.

2) An increase in the lip thickness parameter, L_R, which defines, essentially, the roundness of the external profile around the inlet highlight.

3) A more gradual diffuser area distribution between the inlet throat and diffuser exit.

4) An increase in average throat Mach number to about 0.6 for low contraction ratio inlets and 0.7 for high contraction ratio inlets; however, further increase in throat Mach number reduces the incidence capability.

5) An increase in Reynolds number, as indicated by Fig. 9.

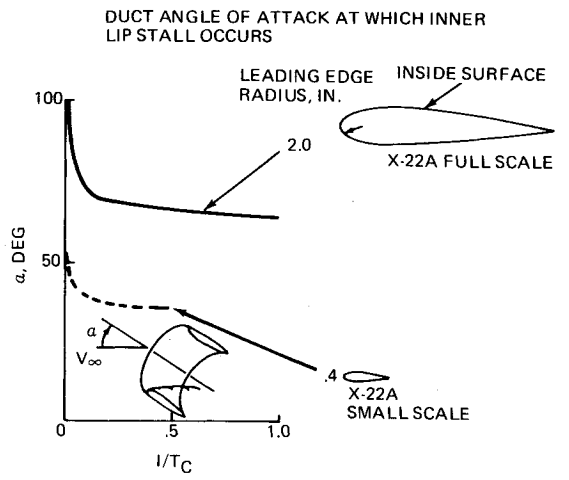

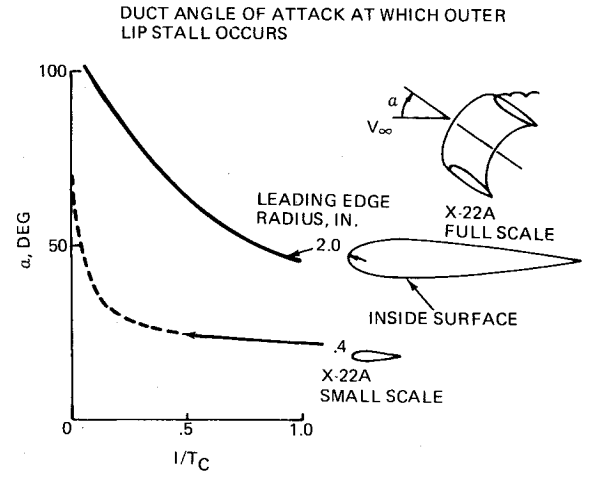

Fig. 9 Reynolds number effect on incidence capability.

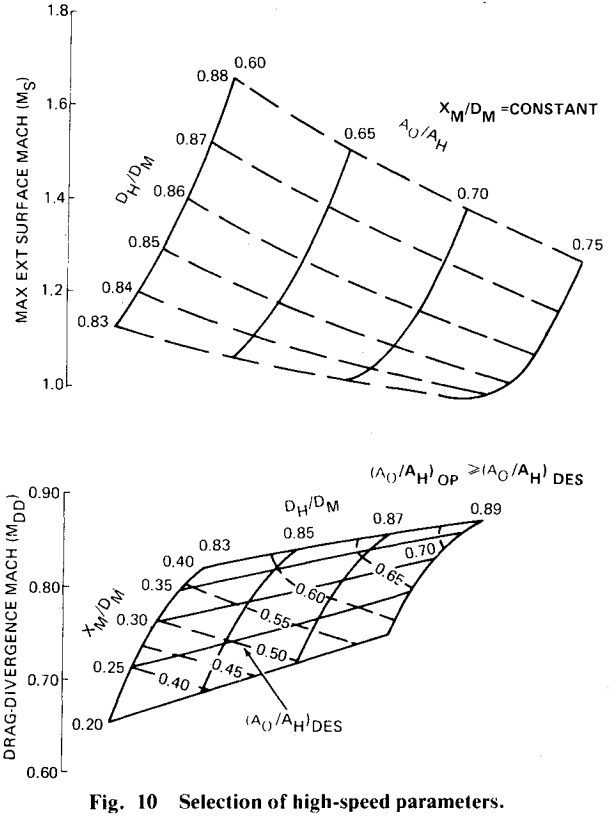

Fig. 10 Selection of high-speed parameters.

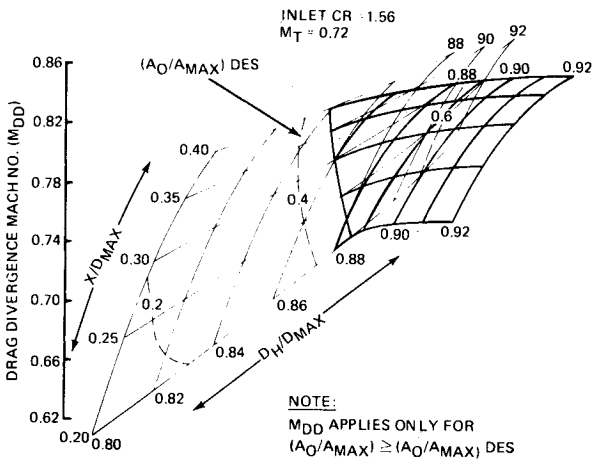

Fig. 11 Drag divergence Mach number suppression.

The inlet must incorporate geometric features consistent with these observations in order to achieve the desired angle-of-attack capability during the critical landing transition.

High Speed

Figure 10 indicates that the drag divergence Mach number of an inlet improves with:

1) An increase in fineness ratio X_M/D_M

2) An increase in diameter ratio, D_H/D_M, provided the operating massflow is equal to, or greater than, the design massflow ratio; otherwise the drag divergence Mach number is suppressed as shown in Fig. 11.

Examination of these low-speed and high-speed correlations indicates that those geometric and flow features which are beneficial to low speed tend to increase drag at cruise. Internally, for example, the selection of a high area contraction ratio for slow-speed considerations reduces the operating massflow ratio of the inlet at cruise, which may give rise to spillage drag; also, the relatively high throat Mach number required at low speed necessitates high diffusion wall angles for a reasonable inlet length. This fact, coupled with high duct velocities, results in total pressure recovery losses and increased distortion. Externally, on the other hand, the generous lip contours required for low speed increase the maximum diameter which affects the geometric cowl parameters, namely the fineness ratio and the diameter ratio, tending to reduce the drag divergence Mach numbers. Consequently, the selection of inlet parameters involves the evaluation of a number of other parameters, such as the effect of design throat Mach number and contraction ratio on maximum diameter and the effect of maximum diameter and operating massflow on external surface Mach number. The proper balance among these parameters is required in order to achieve high total pressure recovery and low distortion, internally, and low drag at cruise.

Inlet Design

The mission requirements of Design 698 were reviewed in conjunction with the above-mentioned correlated data, and two baseline inlets, plus variations, were designed for each of the critical landing configurations shown earlier on Fig. 7. Pertinent inlet parameters are shown in Table 1.

Inlet I_1, the baseline for the critical landing transition with flaps down, was derived from the Ref. 1 inlet of CR of 1.46. Previous analysis, contained in Ref. 2, had indicated that the Ref. 1 inlet of $CR = 1.56$ had adequate incidence capability to meet this transition requirement. Inlet I_1^2 was designed to meet the more severe critical landing transition shown in Fig. 7. The highlight areas of both baseline inlets were circular and parallel to the throat, but displaced downward to result in a

Table 1 Test configurations

Designation	*Area CR* A_H/A_T	Bottom Lip $(R_H/R_T)^2$	Centerbody[b]
Baseline inlet			
I_1	1.46	1.56	Short
I_1^1	1.46	1.56	Long
I_1^2	1.50	1.69	Short
I_1^{21}	1.50	1.69	Long
Scarfed inlet			
I_2	1.36[a]	1.50[a]	Short
I_2^1	1.48[a]	1.67[a]	Long

[a] Inlet I_2 Values are effective. [b] Centerbody Contour: short: 1.6/1 ellipse, long: 3.25/1 ellipse.

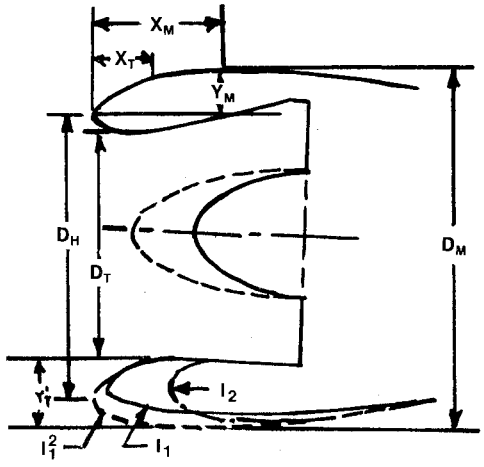

conventional upper lip contraction ratio and a windward bottom lip with the required contraction ratio, namely, 1.56 for inlet I_1 and 1.69 for inlet I_1^2. The scarfed inlet incorporated the bottom lip internal contour of inlet I_1 and was faired externally to the external contours of inlet I_1^2.

All inlets were tested per Ref. 3 at the most critical speed/nacelle angle conditions, but the one most thoroughly investigated was inlet I_1^{21}, which exhibited the best performance and highest angle-of-attack capability.

A complete description of inlet I_1^{21}, hereafter called Design 698 Inlet, is presented in Ref. 4.

Inlet Tests

Model Installation

Each inlet was fitted to a 5.5 in.- (13.97 cm) diam fan and tested in the Grumman 7 × 10-ft (2.13 m by 3.05 m) low speed Wind Tunnel. The tunnel is open-circuit, open-return, continuous-flow with a range of freestream velocities of 0 to 115 knots (0 to 59.3 m/s).

Figure 12 is a photograph of the model installed in the tunnel. Both the isolated nacelle and the reflection plane installations are shown. The model was rotated in the horizontal plane from 0 to 90 deg angle of attack.

Inlet Instrumentation

The main inlet instrumentation was at the fan face and consisted of

1) Eight equally spaced spokes of six total, and one static, pressure probes.This instrumentation was area-weighted to provide fan flow.

2) Two dynamic total pressure transducers located 5 deg on either side of the bottom centerline and at the same radial distance as the total pressure probes near the wall. These transducers were used to determine flow separation and/or flow reattachment.

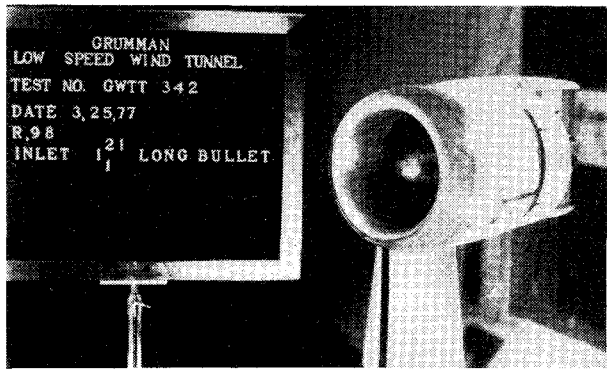

A) ISOLATED

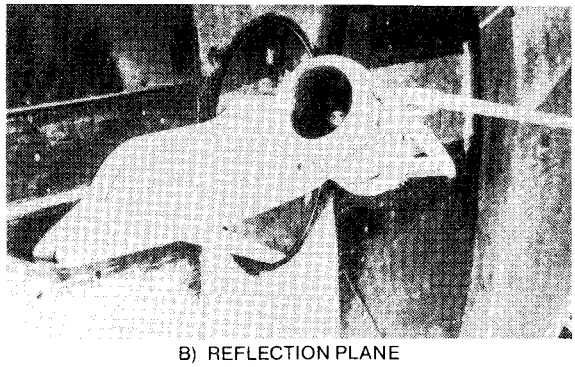

B) REFLECTION PLANE

Fig. 12 Model installation.

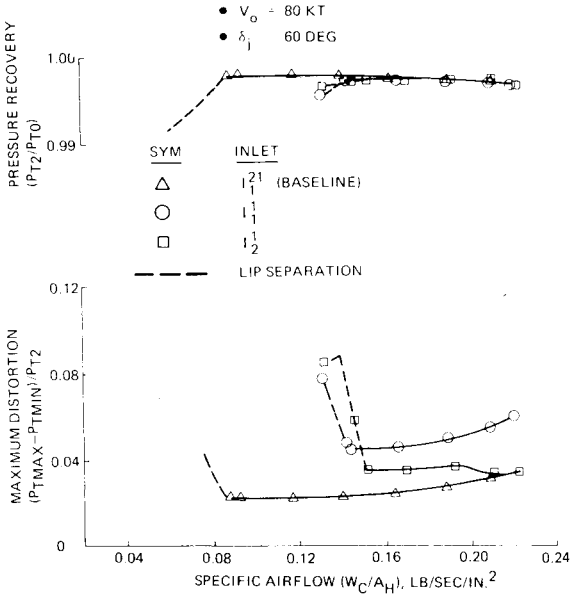

Fig. 13 Inlet performance comparison, V_o = 80 KT.

Inlet duct instrumentation consisted of seven static pressure taps along the centerline of the bottom wall. Protruding instrumentation was not used anywhere in the duct, to avoid extraneous wakes affecting the fan instrumentation measurements.

The outputs from the fan face instrumentation were displayed in the control room for monitoring the test and determining flow separation, in addition to being recorded along with all other measurements for the usual data reduction process.

Test Procedures

Definitions of the inlet performance characteristics and of the flow separation bounds were obtained at constant tunnel

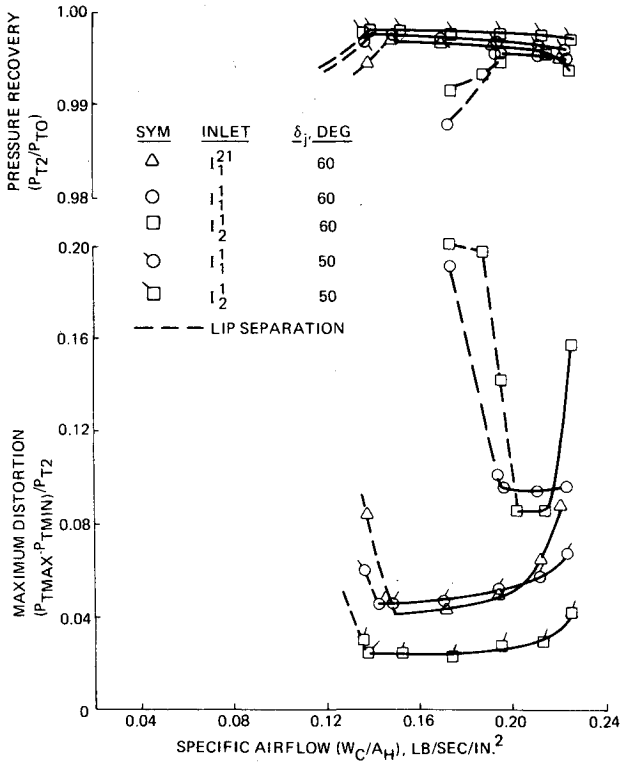

Fig. 14 Inlet performance comparison, $V_0 = 110$ KT.

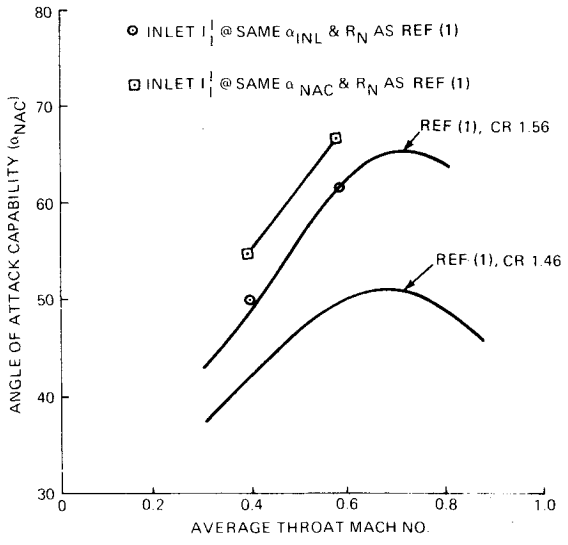

Fig. 15 Separation bounds comparison, $V_0 = 110$ KT.

speed and nacelle inclination by reducing fan speed to the point of incipient separation, inducing separation by further fan speed reduction and then increasing fan speed to reattach the flow. Incipient separation or attachment was approached with very small intervals of fan speed change in order to minimize subjective judgement errors. In the case of reattachment, test experience indicated that sufficient time be allowed for stabilization before recording the data. The fan face total pressure profiles and the dynamic probe traces were continuously monitored.

The observed data were subsequently analyzed in conjunction with plots of the pressure recovery, the maximum distortion and the lower lip static pressure distributions. It will be shown later, in the discussion of the test results, that the observed phenomena of separation and attachment were in excellent agreement with definite concurring changes in the

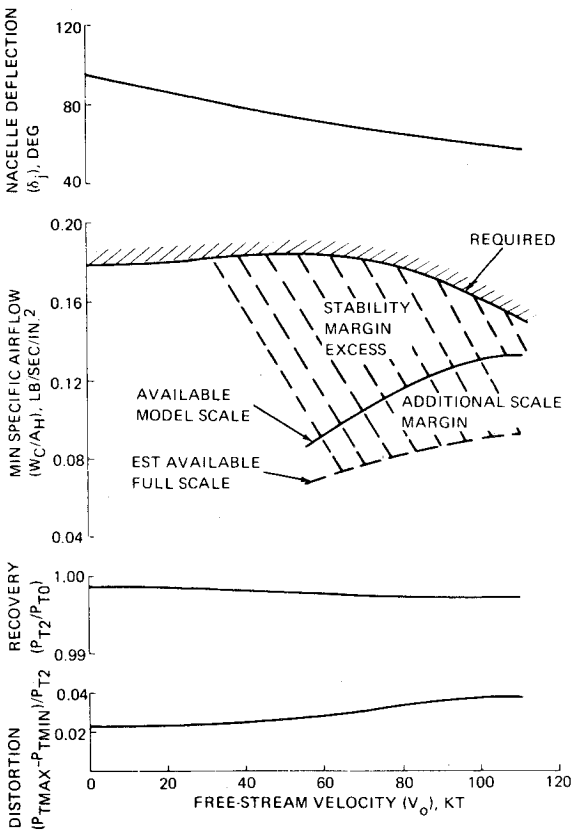

Fig. 16 Critical landing transition matched performance.

total pressure recovery, the maximum distortion parameter and the lower lip static pressure distribution.

Having determined the envelopes of incipient separation (minimum stable operating point approached from stable conditions) and of attachment (minimum stable operating point approached from unstable conditions), they were verified by a second test method: holding tunnel and fan speeds constant and increasing nacelle inclination to induce separation, and then decreasing nacelle inclination to reattach. The same stabilization and recording procedure was used in approaching these phenomena as was used for the previous method.

Test Results

Comparative Inlet Performance

The isolated inlet performance of the various test inlets is compared in Figs. 13 and 14 at conditions of high forward speed/nacelle angle combinations. As expected, Design 698 inlet has substantially more stability margin and lower distortion levels than the other inlets, since it was designed to meet the more severe, no-flaps, critical landing transition. The other two inlets, I_1^1 and I_2^1, also performed as expected, considering that they were intended to meet the less critical landing transition of an aircraft configuration employing flaps. In fact, inlet I_1^1, derived from the Ref. 1 inlet of *CR = 1.46,* performed as well as the *CR* 1.56 inlet, thus corroborating the analytical results of Ref. 2. The comparison between Inlet I_1^1 and the Ref. 1 inlets is shown in Fig. 15.

Design 698 Inlet

The isolated inlet performance characteristics for forward speeds up to 110 KT (Mach 0.17), and at various nacelle deflections, δ_j, have been presented and discussed in Ref. 4. In summary, stable inlet/engine matching at very high pressure recoveries and low levels of distortion are obtainable for low speed flight modes. During takeoff at a nacelle deflection, δ_j, of 50 deg, total pressure recoveries better than

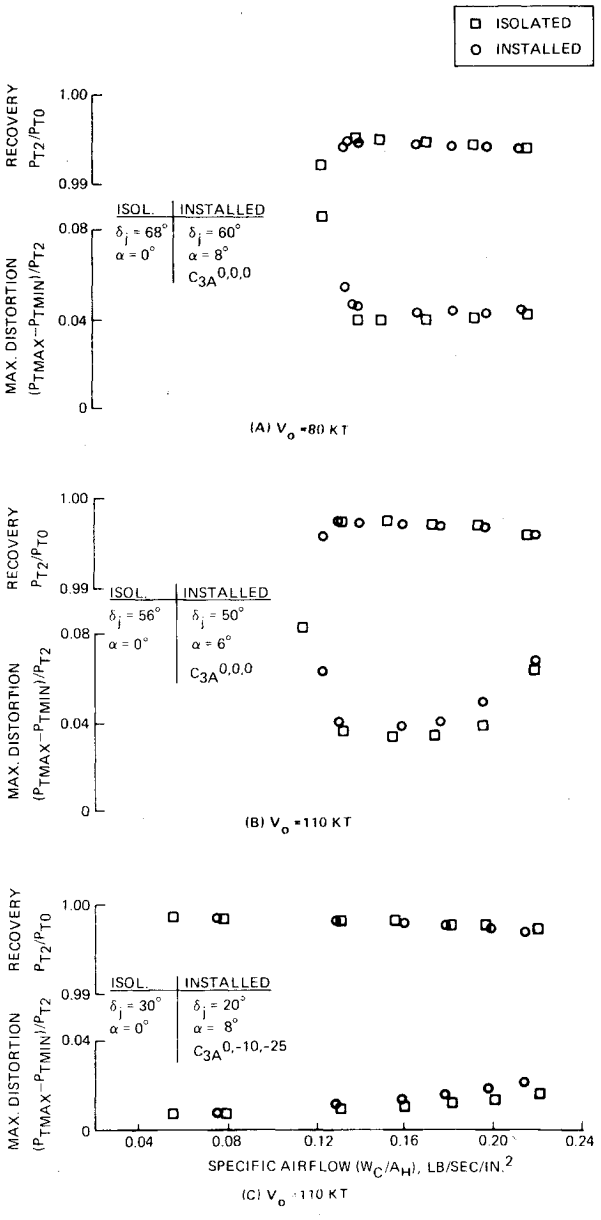

Fig. 17 Forebody interference effects.

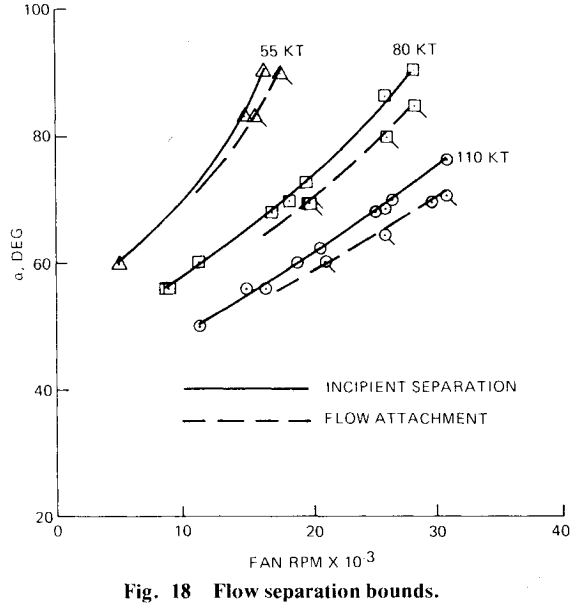

Fig. 18 Flow separation bounds.

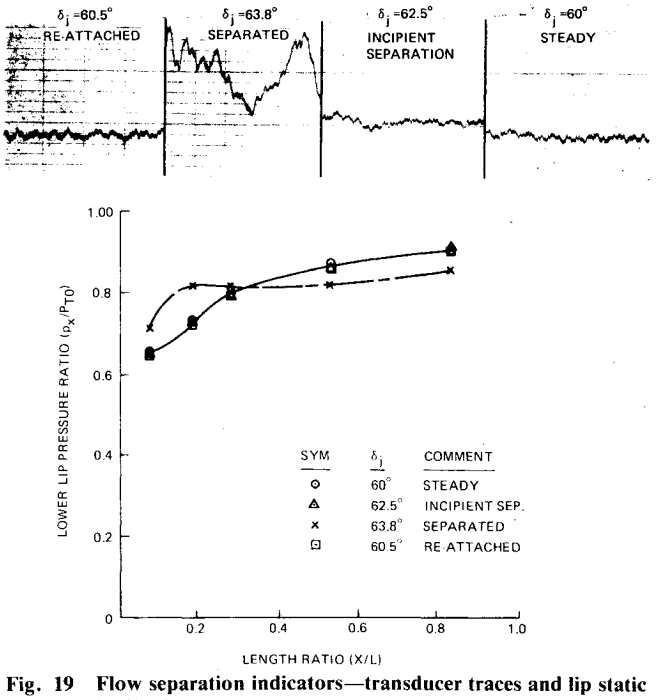

Fig. 19 Flow separation indicators—transducer traces and lip static pressure distributions.

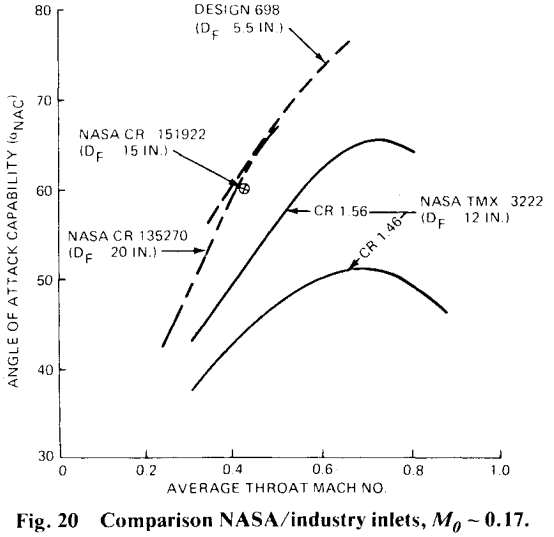

Fig. 20 Comparison NASA/industry inlets, $M_0 \sim 0.17$.

0.996 and distortions less than 4.0% were obtained to the highest forward speed of 110 KT (Mach 0.17).

The matched inlet performance during the critical landing transition is shown in Fig. 16. Even in this severe environment, the inlet operates at total pressure recoveries better than 0.996 and distortions less than 4.0% throughout transition. Additionally, the inlet has substantial stable range to operate efficiently at even more severe inflow environments than required by the most critical landing transition requirement of Design 698, especially when the full-scale capability of the inlet (shown dashed on specific airflow plot) is considered. The full-scale estimates are based on correlations of NASA and industry data. Installed inlet performance was obtained at critical forebody/nacelle positions during the landing transition. Figure 17 compares the installed and the isolated performance at the same inlet orientation relative to the freestream. The data indicates that, for the aircraft angles of attack and canard positions shown, the forebody flow effects on inlet perfomance are almost negligible.

Flow Separation Bounds

Figure 18 summarizes the incipient separation (open symbols) and reattachment bounds (flagged symbols) at the test freestream velocities of 55 KT (28.4 m/s), 80 KT (41.2 m/s) and 110 KT (56.7 m/s). Included are all data, whether obtained by varying fan speed at constant freestream velocity and angle of attack or by varying angle of attack at constant freestream velocity and fan speed. The trends indicate close agreement between the two methods of defining the inlet separation and attachment bounds. In general, the hysterisis effect (difference in angle between separation and reattachment) increases with fan speed at a given freestream velocity and with freestream velocity at a given fan speed.

It must be emphasized here that, as defined in this paper, the incipient separation and reattachment points represent stable inlet airflow condtions with no degradation in the inlet performance parameters as proven by the typical transducer traces and static pressure distributions shown in Fig. 19. The transducer shows increased activity and the pressure distribution indicates a definite change, only when the inlet is forced well into the separated regime; at incipient separation and reattachment, the transducer traces and the static pressure distributions are identical to those of the steady case.

The flow separation bounds of the Design 698 inlet are compared with available NASA and industry data in Fig. 20. The Design 698 inlet achieves higher angles of attack than all these high contraction ratio inlet types even though tested at a smaller Reynolds number than the others. This performance is attributerd to the unique features incorporated by judicious selection of the low-speed parameters that maximize angle-of-attack capability.

Planned Development

The high contraction ratio and generous external contours required for high angle-of-attack capability at low speed tend to make the nacelle bulky, heavy and draggy. It would be desirable, therefore, to try to meet the low-speed requirements with shorter and more slender nacelles by either trading off excess stability margin or investigating alternative means of forestalling flow separation in the inlet. To explore these possibilities a cooperative effort between Grumman and NASA/LeRC has been initiated, and tests are now in progress at NASA/Lewis to investigate offshoots of the Grumman designs with both passive and active flow attaching devices, such as leading edge slats, vortex generators, blowing slots and suction, in order to optimize an inlet system between low-speed and cruise requirements at minimum inlet length, weight and complexity.

References

[1] Miller, B.A., Dastoli, M.J., and Wesoky, H.L., "Effect of Entry – Lip Design on Aerodynamics and Acoustics of High-Throat-Mach-Number Inlets for the Quiet, Short-Haul Experimental Engine," NASA TM X-3222, May 1975.

[2] Potonides, H.C., "Design 698-305 Baseline Inlet for the Allison T-701/Hamilton Standard 76-inch Q-Fan Engine," Grumman Aerospace Corp. PDM-698-11, Sept. 27, 1976.

[3] Potonides, H.C., "Type A V/STOL Inlet Development. Low Speed Wind Tunnel Test, GWTT 342," Grumman Aerospace Corporation, March 1977.

[4] Potonides, H.C., "Development of an Inlet for a Tilt Nacelle Subsonic V/STOL Aircraft," ASME 78-GT-121, April 1978.